

A SURVEY OF H I IN SEYFERT GALAXIES

TIMOTHY M. HECKMAN, BRUCE BALICK, AND WOODRUFF T. SULLIVAN III

Department of Astronomy, University of Washington, Seattle

Received 1978 January 3; accepted 1978 March 21

ABSTRACT

We report observations of neutral hydrogen for some 58 Seyfert and Seyfert-like galaxies, most with redshifts less than 0.033 (10,000 km s⁻¹). H I emission was detected in 25 galaxies, and H I absorption in three. Relative to normal galaxies of the same morphological type, one-third of the detected Seyferts exhibit strong anomalies in their H I properties, whereas about two-thirds appear normal. These anomalies include extreme values of $\mathfrak{M}_{\text{H I}}/L_{\text{pg}}$, broad and complex profiles, and absorption lines. Anomalous H I properties appear to be correlated with large nuclear luminosities. A comparison of nuclear (optical) and H I (radio) systemic redshifts shows no systematic differences in the mean, although the dispersion of optical-H I velocities is larger for these Seyfert galaxies than for normal galaxies.

Crude maps of the H I in NGC 1068, NGC 3227, NGC 4670, and Mrk 348 have been made. In NGC 1068 the H I rotation axis is perpendicular to the minor axis of the main galaxy and is aligned along the minor axis of an outer ring. The gas in NGC 3227 appears to be disrupted, probably because of the companion galaxy NGC 3226. Mrk 348 is characterized by H I that is extended 3-4 times its optical diameter. Possible communication between the disk and active nucleus is explored, and a scenario for the evolution of Seyfert activity is presented.

Subject headings: galaxies: Seyfert — radio sources: 21 cm radiation

I. INTRODUCTION

Seyfert galaxies have received increasing astronomical interest because of their probable status as transition objects between normal galaxies and most types of quasars. While most of the previous attention has focused on their nuclear properties, it is currently felt that the energy of the nucleus can derive, at least in part, from gravitational energy of the disk. Consequently, we have undertaken observations of the properties of the gaseous component, specifically the H I in the disk, in order to better understand the relationship of disk and nucleus.

The disks of Seyfert galaxies remain largely unexplored. Adams (1977) has investigated the stellar distribution through deep photographs in the violet. It is the gas, however, and not the stars, which would be expected to exhibit the most sensitive indication of hydrodynamic energy exchange with the nucleus. A first attempt to map the H II distribution of a Seyfert galaxy (by H α photography) by Simkin (1975) showed a puzzling absence of H II emission in the inner several kiloparsecs of NGC 4151. From this observation, and by analogy to normal galaxies, it is reasonable to expect that most of the mass of the gaseous part of the disk is neutral hydrogen.

It has been several years since H I observations of Seyfert galaxies have been reported (e.g., Lewis and Davies 1973; Davies 1973). These observations included a total of about a half-dozen galaxies, all of them relatively nearby. Instrumentation has advanced significantly in the interim, and the cosmological volume in which Seyfert galaxies should now be detectable has increased about an order of magnitude.

For these reasons we have undertaken a survey of some 58 Seyfert or Seyfert-like galaxies, which included virtually all of the approximately 40 known Seyfert galaxies with recession velocities less than about 10,000 km s⁻¹ and north of declination -20° . It is our intention to identify galaxies of exceptional interest, and also to draw statistical inferences about the similarities and differences between the disks of Seyfert galaxies and their counterparts in "normal" galaxies.

Herein we present observations of the integral H I properties of Seyfert galaxies. Additionally, results of a few crude H I maps made on four relatively large galaxies are reported. These findings comprise the first of a coordinated series of radio and optical surveys which will concentrate on nonnuclear properties of active galaxies.

II. OBSERVATIONS

Observations were undertaken on the 91 m transit telescope of the National Radio Astronomy Observatory (NRAO)¹ during 1976 October and 1977 February, and on the 305 m spherical telescope of the National Astronomy and Ionosphere Center (NAIC)² at Arecibo during 1977 March and September.

A movable feed on the 91 m telescope makes it possible to track objects with about 97% optimum efficiency for 4/cos (declination) minutes per day. A new dual-channel receiver tunable from ~ 1000 to

¹ The NRAO is operated by Associated Universities, Inc., under contract with the National Science Foundation.

² The NAIC is operated by Cornell University under contract with the National Science Foundation.

1450 MHz and with a system temperature of ~ 45 K was employed on the 91 m telescope in conjunction with the model III autocorrelator. Each receiver was connected to dipole feeds of orthogonal linear polarization. The spectral line system was configured as two 10 MHz, 192-channel spectrometers, each connected to different front-end receiver channels. The data were calibrated and averaged using standard software available at the NRAO. The final averages have been smoothed over three channels (33 km s^{-1} velocity resolution), and a linear baseline (or, in a few cases, a linear plus sinusoidal baseline) has been

fitted and removed. The absolute calibration of the H I fluxes is uncertain by about 10%.

Each galaxy was observed on at least 10 days by subtracting from on-galaxy observations the spectrum of a cold sky position (OFF spectrum) obtained in an identical manner and which immediately preceded or followed the on-galaxy observations. This procedure usually acceptably removes systematic spectral-baseline curvature common to both the ON and OFF observations. In some cases subtraction of the ON and OFF observations does not completely eliminate spectral-baseline curvature. This situation generally arises

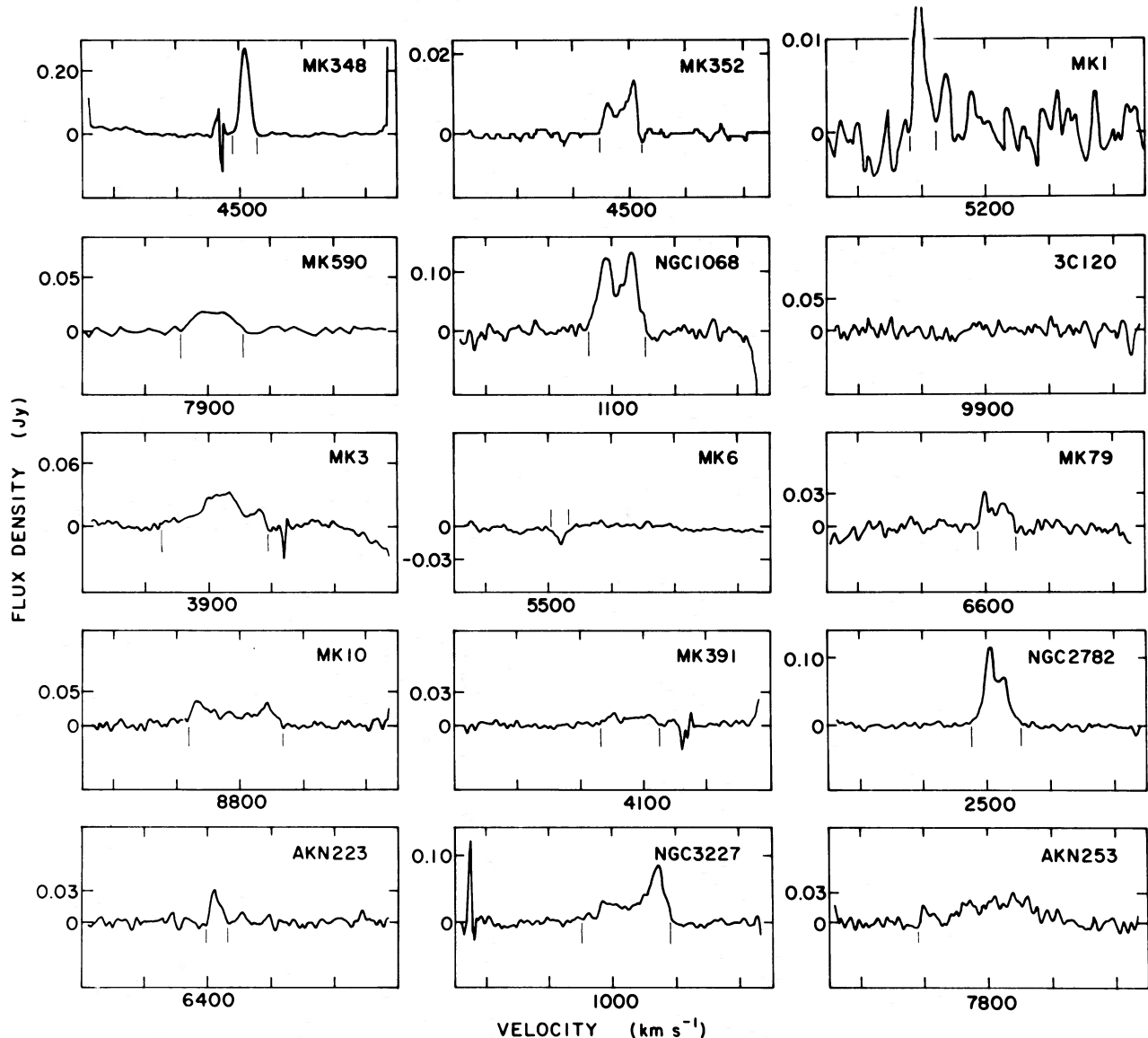


FIG. 1.—Spectra of detected and significant undetected galaxies. The scales are in Jy ($\equiv 10^{-26} \text{ W m}^{-2} \text{ Hz}^{-1}$) and km s^{-1} . The horizontal scale has a reference velocity (cz) indicated under its tick mark and other tick marks spaced every 400 km s^{-1} . For detected galaxies, the tick marks directly under the profile indicate the extent of the line as listed in Table 1. Unsubtracted galactic hydrogen appears between -200 and 200 km s^{-1} . Spikes between 4300 and 4400 km s^{-1} result from variable receiver interference and should be ignored.

if the continuum radiation from the observed galaxy exceeds ~ 0.1 Jy or if a strong continuum source (such as the Sun) is present in the beam sidelobes. Any such residual curvature arising from nonsolar sources of flux less than 1 Jy can be accurately fitted to a sinusoid and removed. Spectra affected by the Sun (which included a large percentage of all daytime data) or by strong continuum sources could not be accurately calibrated and are not included in this study.

Because their sizes are comparable to the $10'$ diameter of the 91 m telescope beam, NGC 1068, NGC 3227, NGC 4051, and NGC 4151 were also observed on the NRAO 43 m telescope. The data acquisition and calibration procedures used to reduce the data are essentially identical to those described above. Integrated H I data given for these four galaxies are based on the 43 m observations.

The Arecibo observations were conducted in a manner similar to the NRAO procedure. A line feed (tuned to 1398 MHz with a 3 dB bandwidth of ~ 40 MHz) was used which illuminates about half of the dish surface. With minor exceptions, off-source observations were made with the same dish-sky geometry as the on-source observations. A dual-channel spectrometer consisting of 252 channels covering a 10 MHz bandpass was used in conjunction with two radiometers connected to feeds of opposite circular polarization. The ON-OFF pairs were subtracted and corrected for changes in antenna gain (varying with zenith angle) and for frequency-dependent line-feed efficiency. The pairs were then stacked and a linear baseline removed. Because of uncertainties in the various efficiency corrections and the noise tube calibration, the absolute fluxes of the

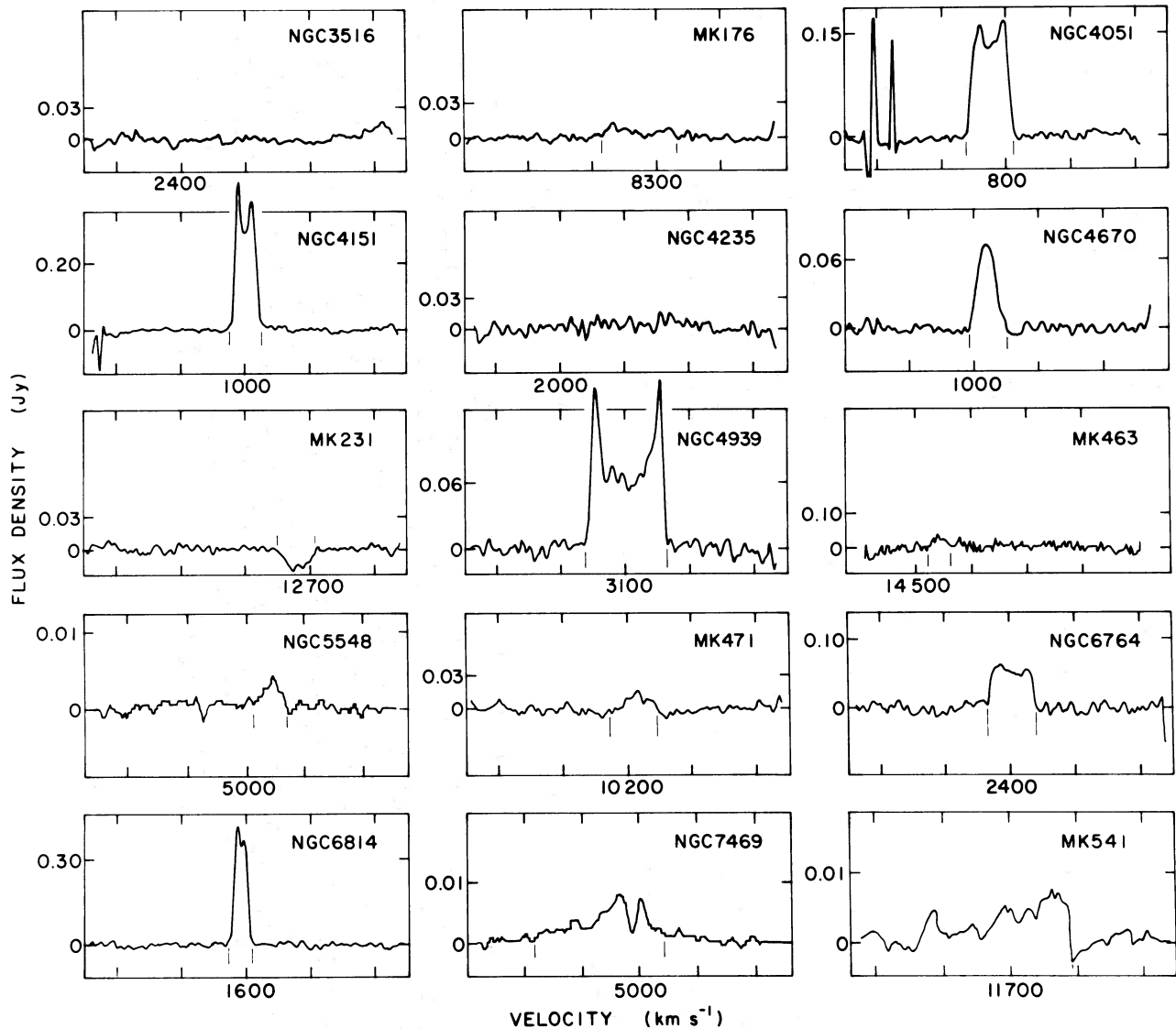


FIG. 1.—Continued

TABLE 1
PROPERTIES OF PROGRAM GALAXIES (fluxes in Jy and velocities in km s⁻¹)

1. Galaxy	2. RA/Dec (1950)	3. $\Sigma \Delta v$	4. Δv_{obs}	5. Δv_{tot}	6. V_{opt}	7. V_{HI}	8. B_{T1}	9. $M_{HI}/10^9 M_{\odot}$	10. $L_{pg}/10^9 L_{\odot}$	11. $M_I/10^9 L_{\odot}$	12. M_{HI}/L_{pg}	13. M_{HI}/M_I	14. M_I/L_{pg}	15. T	16. $S_{1.415}$	17. Profile
III Zw2 (91)	0008+10	<1.2			26930		15.1 (Z)	<122	370		<.33			pec	.26	
MK 348 (91)	0046+31	17.6±1.8	145		4700	4534	15.1 (M)	34	10.5		3.3	0.03		0	.3	lps
MK 352 (305)	0057+31	1.9±.4	245	400	4477	4448	14.6 (M)	3.2	16.5	108	0.20	0.03	6.5	-2	.08	2pa
MK 1 (305)	0113+32	0.7±.3	150	220	4793	4780	14.6 (R)	1.8	18.0	57	0.10	0.03	3.2	pec	.08	lps
MK 358 (91)	0123+31	<3.0			13750		15.0 (ZM)	<53	106		<.5			4		
MK 590 (91)	0212-01	5.2±1.4	380	1010	8100	7910	14.1 (ZM)	30	85	2070	0.35	0.014	24	1		lps?
NGC 985 (91)	0232-09	<0.8			12950		13.8 (R)	<13	285		<.04			ring		
NGC 1068 (91)	0240-00	28.9±2.9	355	670	1109	1140	9.2 (R)	3.5	152	600	0.02	0.006	4.0	3	4.9	2ps
III Zw55 (91)	0338-01	<1.5			7380		14.3 (Z)	<7.7	61		<.13			-5		
3C 120 (91)	0430+05	<2.3			9900		13.6 (R)	<22	200		<.11			-2	5.6	cpx
MK 3 (91)	0609+71	9.5±2.2	680	1450	4054	3952	14.2 (ZM)	14.3	227	3430	0.53	0.004	127	-2	1.2	abs.
MK 6 (91)	0645+74	<1.4			5660		14.8 (ZM)	<4.6	41		<.11			-1	.32	
MK 374 (91)	0653+54	<1.6			13200		14.8 (M)	<26	123		<.21			3	.013	
MK 376 (91)	0710+45	<1.9			16800		15.3 (M)	<50	120		<.42			3		
MK 79 (91)	0738+49	4.0±1.0	225		6598	6643	13.1 (R)	16.5	142		0.12	0.07	4.2	3	.019	2pa
MK 10 (91)	0743+61	12.0±3.0	625	680	8685	8753	12.9 (R)	86	297	1250	0.25	0.07		3		2ps
MK 382* (91)	0752+39	<1.5			10200		15.0 (ZM)	<15	59		<.025			4		2ps?
MK 391* (91)	0851+39	2.7±1.4	365	505	3979	3992	14.1 (M)	4.0	20	280	0.40	0.015	14	1	.11	2pa
NGC 2782* (91)	0910+40	15.9±1.6	335	500	2537	2562	11.8 (M)	9.8	70	410	0.14	0.02	5.9	1		
MK 110 (91)	0921+52	<1.0			10800		15.5 (M)	<11	41		<.27			pec	.01	
Zw0934+01 (91)	0934+01	<1.7			15550		14.9 (Z)	<39	149		<.26			3		
AKN 223* (91)	0954+07	2.2±0.9	125	155	6600	6518	14.5 (Z)	8.9	38	20	0.23	0.43	0.5	0		lps
MK 142 (91)	1018+51	<1.5			13500		16.0 (M)	<26	41		<.63			-2		
NGC 3227 (91)	1020+20	20.0±2.8	575	800	1152	1106	11.2 (R)	2.4	24	670	0.10	0.004	28	1	.016	2pa
MK 34 (91)	1030+60	<1.5			15300		15.4 (M)	<33	91		<.36			0		cpx
AKN 253* (91)	1041-01	8.6±4.5	745	910	7800	7808	13.6 (Z)	50	126	860	0.40	0.06	6.8	0	.022	
NGC 3516 (91)	1103+72	<1.4			2540		12.1 (R)	<1.0	63		<.02			-2		
MK 40 (91)	1122+54	<2.2			6150		14.4 (M)	<8	37		<.21			-2		
MK 176 (91)	1129+53	2.0±1.4	485	485	8080	8208	14.2 (M)	12.8	79	180	0.15	0.08	2.3	2	.021	2ps
MK 42 (91)	1151+46	<1.2			7200		15.6 (R)	<6	17		<.34			2	.02	2ps
NGC 4051 (91)	1200+44	35.9±3.6	295	480	674	701	10.7 (R)	1.7	15	140	0.12	0.01	9.6	4	.006	
MK 198* (91)	1206+47	<0.8			7220		14.6 (R)	<4	42		<.09			-2		
NGC 4151 (91)	1208+39	47.1±4.7	200	295	970	994	11.9 (R)	<1.3	27	85	0.16	0.05	3.1	1	.35	2ps
NGC 4235 (91)	1214+07	<2.4			2410		15.1 (M)	<6	57		<.02			1		
MK 50 (91)	1220+02	<1.4			6910		15.2 (M)	<100	24		<.26			-2		
NGC 4670* (91)	1242+27	9.6±0.7	245	380	1159	1084	13.8 (R)	1.1	5	48	0.22	0.02	9.6	0	.011	lps
MK 231 (91)	1254+57	<1.5			12430		13.9 (R)	<21	234		<.09			5	.29	abs.
NGC 4939* (91)	1301-10	45.2±4.5	520	605	3096	3109	11.6 (R)	41	125	1020	0.33	0.04	8.2	4	.016	2ps
MK 270* (91)	1339+67	<0.8			2700		14.5 (M)	<.55	8.5		<.06			pec	.15	
MK 273* (91)	1342+56	<8.3			11460		14.0 (R)	<100	184		<.55			-2	.021	
MK 279 (91)	1351+69	<2.9			9220		14.5 (ZM)	<23	75		<.31			-2		
MK 463 (91)	1353+18	6.0±2.3	160	210	15140	14702	15.0 (ZM)	124	129	190	0.96	0.65	1.5	3	.34	lps
NGC 5548 (305)	1415+25	0.5±0.15	160	325	4981	5204	12.8 (R)	1.1	108	180	0.01	0.006	1.7	0	.027	lps, abs.
MK 471* (91)	1420+33	1.2±0.7	305	405	10132	10256	15.0 (M)	12.5	59	310	0.21	0.04	5.2	1	.033	lps
MK 474 (91)	1433+48	<1.0			12300		15.2 (ZM)	<14	71		<.2			0		
MK 290 (91)	1533+58	<1.1			9240		14.7 (R)	<9	63		<.14			-5	.005	
MK 291 (305)	1553+19	<2.6			10500		14.5 (M)	<27	97		<.28			1		
MK 298 (91)	1603+17	<0.8			10230		15.2 (M)	<8.4	50		<.17			pec	.004	
MK 501* (91)	1652+39	<4.3			10000		13.1 (ZM)	<40	323		<.13			pec	1.45	
MK 504 (91)	1659+29	<1.2			10800		15.8 (R)	<13	31		<.42			-1		
MK 506 (91)	1720+30	<1.6			12900		14.8 (ZM)	<25	113		<.22			-2		
MK 507* (91)	1748+68	<2.5			15900		15.4 (M)	<59	98		<.61			-2		
NGC 6764 (91)	1906+50	15.1±2.1	300	365	2412	2412	12.2 (Z)	8.2	43	134	0.19	0.06	3.1	3	.19	2ps?
NGC 6814 (91)	1936-10	33.7±3.4	145		1403	1560	11.1 (R)	7.8	50		0.16			4		2pa
II Zw136 (91)	2130+09	<1.9			18510		13.8 (Z)	<61	582		<.10			pec		
NGC 7469 (305)	2300+08	3.1±0.6	885	1300	4894	4754	12.2 (R)	6.3	168	2450	0.04	.003	14.6	1	.35	cpx
NGC 7603 (91)	2316-00	<2.3			8800		13.9 (Z)	<17	120		<.14			3	.034	
MK 541 (91)	2353+07	2.1±1.2	1050	1495	12300	11716	15.0 (M)	28	77	3980	0.01	.28	52	2		cpx

TABLE 2
H I ABSORPTION LINES

Galaxy	τ_{HI}	N_{HI} (10^{20} cm^{-2})	V_{abs} (km s^{-1})	ΔV_{abs} (km s^{-1})
Mrk 6	0.04	7.9	5594	100
Mrk 231	0.05	18.0	12634	240
NGC 5548	0.14	4.7	4754	35

Arecibo data are accurate to only 20%. Measurements of the H I flux of unresolved galaxies common to the 91 m and 305 m programs corroborate the expected accuracies.

III. OBSERVATIONAL RESULTS

Results of the observations are summarized in Tables 1 and 2 for the Seyfert galaxies included in the present program. Figure 1 includes spectra of all detected galaxies and significant undetected galaxies. A description of Table 1, which includes emission-line parameters and upper limits for emission, follows:

Column (1).—Galaxy designation. An asterisk denotes a questionable classification as a Seyfert Galaxy. In general, these questionable Seyferts are galaxies which have been classified as a Seyfert galaxy in the literature but which do not appear in the catalog of Seyfert galaxies by Weedman (1977). MK denotes a Markarian (Mrk) designation. The diameter of the telescope used to obtain the data is also indicated.

Column (2).—Abbreviated right ascension and declination (1950).

Column (3).—Integrated H I flux and error or upper limit. The quoted uncertainties and upper limits are computed from the greater of the calibration uncertainty (as described above) or the channel-to-channel rms (typically 2 mJy for the 91 m telescope) multiplied by the observed (or expected) line width. Expected line widths are estimated by assuming an intrinsic line width of 600 km s^{-1} (approximately the average for the detected galaxies) and correcting for galaxy inclination. It is not clear (see below) that an inclination correction is appropriate in every case.

Column (4).—Full profile width at zero intensity ($\Delta v_{\text{obs}} \equiv c\Delta z_{\text{obs}}$). Many of these estimates are necessarily somewhat subjective, especially for galaxies with low-intensity wings.

Column (5).—Line width corrected for inclination, Δv_{tot} (following Roberts 1975). Values for the inclination angle are derived from the ratio of major to minor axis given in the *Reference Catalogue of Bright Galaxies* (de Vaucouleurs, de Vaucouleurs, and Corwin 1976, hereafter RCBG) wherever possible. Other ratios of major to minor axis were estimated visually from the E plates of the Palomar Sky Survey (PSS). Values for Δv_{tot} are not given for face-on galaxies with inclinations less than 20° . The inclination correction presupposes the H I to be coplanar with the galaxy and in circular motion around the galactic nucleus. These assumptions should be regarded with

skepticism for active galaxies because of the possibility that the H I is disrupted by the nuclear activity. Five of our H I profiles definitely show asymmetries indicative of noncircular motions, and a correction for inclination is clearly not appropriate in these cases. Such galaxies are indicated by a colon in this column.

Column (6).—Published heliocentric optical velocity ($v_{\text{opt}} \equiv cz_{\text{opt}}$). The entries are based on values of v_{opt} or z from Khachikian and Weedman (1974), RCBG, Adams (1977), or Weedman (1977). The redshift of NGC 4235 was supplied from Lick scanner observations by D. Jenner (private communication). The optical velocity of Mrk 1 given by Khachikian and Weedman was kindly confirmed by D. E. Osterbrock (private communication), and that of Mrk 348 was measured by Koski (1976).

Column (7).—Measured heliocentric H I velocity ($v_{\text{HI}} \equiv cz_{\text{HI}}$). Each entry is an average of the velocity determined in two ways. One velocity is the average of the two extreme velocities at which the line profile falls to 20% of its peak value. The second is the first velocity moment $\bar{v} = \sum_n [v_n S(v_n)] / \sum_n S(v_n)$, where $S(v_n)$ is the line profile flux density function in channel n . The two methods generally differ by only $10\text{--}20 \text{ km s}^{-1}$, but by more if the line profile is asymmetric. Errors in the determination of channel velocity are negligible ($\sim 0.1 \text{ km s}^{-1}$).

Column (8).—Total corrected photographic apparent magnitude. The values are based on RCBG measurements wherever possible. The RCBG measurements have been corrected for Galactic absorption, internal absorption, and redshift. Magnitudes from sources other than the RCBG have been corrected by following the precepts of the RCBG. The other sources are the Markarian survey (Markarian 1967, 1969a, b, 1973; Markarian and Lipovetsky 1971, 1972, 1973, 1974) and the *Catalogue of Galaxies and Clusters of Galaxies* (Zwicky and Herzog 1963).

The uncertainties of the photographic magnitudes quoted in the RCBG are typically less than ~ 0.1 mag. Where possible, we have compared magnitudes from the RCBG on the one hand and the Markarian and Zwicky lists on the other. We find that the magnitudes of the latter sources typically differ from those of the RCBG by ~ 0.5 mag separately, or by ~ 0.3 mag in tandem. We identify the source of the entry by R, M, and Z for the RCBG, Markarian, and Zwicky compilations, respectively.

Column (9).—The integrated hydrogen mass as given by

$$M_{\text{HI}}/M_{\odot} = 94v^2 \left(\frac{50}{H_0}\right)^2 \Delta v_{\text{ch}} \sum_n S(v_n), \quad (1)$$

where v is the systemic redshift in km s^{-1} ; $S(v_n)$ is in units of Jy; the channel width Δv_{ch} is in km s^{-1} ; and H_0 is the Hubble constant, taken as $50 \text{ km s}^{-1} \text{ Mpc}^{-1}$.

We note the early suggestion by Roberts (1975) that H I emission from highly inclined galaxies (axial ratio less than or equal to 0.25) may suffer some internal absorption. This conclusion was based on his measured dependence of the H I mass to photographic

luminosity ratio $\mathfrak{M}_{\text{HI}}/L_{\text{pg}}$ on inclination. Since then, however, different inclination corrections to the photographic magnitudes M_{pg} have been derived (Shostak 1975; RCBG; Balkowski 1973). It thus appears that the dependence of $\mathfrak{M}_{\text{HI}}/L_{\text{pg}}$ is best explained by the newer extinction corrections to M_{pg} rather than by any internal H I absorption, and we have applied no correction for internal H I absorption to the entries in the table.

Column (10).—The total photographic luminosities L_{pg} determined from the photographic magnitudes and a Hubble distance computed from v_{HI} (or, for the undetected galaxies, v_{opt}) and $H_0 = 50 \text{ km s}^{-1} \text{ Mpc}^{-1}$. The statistical uncertainties in L_{pg} range from 10% to 60%. These errors derive from measurement errors of M_{pg} and ignore uncertainties associated with the value of H_0 .

Column (11).—The total or indicative mass \mathfrak{M}_i , computed according to the formula

$$\mathfrak{M}_i/\mathfrak{M}_\odot = 2.91v\theta\Delta v_{\text{tot}}^2, \quad (2)$$

where a value of $H_0 = 50 \text{ km s}^{-1} \text{ Mpc}^{-1}$ is assumed ($\mathfrak{M}_i \propto H_0^{-1}$). Here v is in km s^{-1} , θ is the corrected diameter of the galaxy in arcsec, and Δv_{tot} is the line profile width listed in column (5). Values of θ are set equal to the quantity $D(0)$ if listed in the RCBG. Otherwise, they are determined by transforming the maximum diameter of the galaxy (as measured on the PSS) to the RCBG system. This transformation is based on PSS measurements of those Seyferts for which $D(0)$ is given in the RCBG.

The values of \mathfrak{M}_i may be seriously in error for several reasons. First, Δv_{tot} is only poorly estimated because of the uncertain correction for inclination. Second, values of θ , especially in those cases where no data are available from the RCBG, are accurate to at best 25%. Moreover, the determination of θ even for bright nearby galaxies is confused because of the frequent association of luminous outer rings with Seyfert galaxies (van den Bergh 1975a). Finally, the applicability of equation (2) is doubtful because its derivation assumes the H I to be moving in bound, circular, and coplanar orbits within the galactic disk, as well as a typical H I mass-radius relation. Owing to the asymmetric line profiles and abnormal $\mathfrak{M}_{\text{HI}}/L_{\text{pg}}$ ratios found in many Seyfert galaxies, these assumptions are very dubious. Perhaps only in the case of "normal" line profile shapes and $\mathfrak{M}_{\text{HI}}/L_{\text{pg}}$ ratios can \mathfrak{M}_i optimistically be deemed accurate within a factor of 2, and then only if the distance to the galaxy is known.

Column (12).—The $\mathfrak{M}_{\text{HI}}/L_{\text{pg}}$ ratio, determined from columns (8) and (9). This quantity is independent of the assumed distance to the galaxy. No attempt to correct L_{pg} for contributions from the nucleus or an outer ring has been made for these entries. Note that as much as half of the total optical luminosity can originate in the nucleus of a Seyfert galaxy, while the H I is generally associated with the disk or in one case, possibly, with an outer ring (NGC 1068).

Column (13).—Fractional H I mass $\mathfrak{M}_{\text{HI}}/\mathfrak{M}_i$, from

columns (9) and (11). See remarks above concerning the accuracy of \mathfrak{M}_i .

Column (14).—The $\mathfrak{M}_i/L_{\text{pg}}$ ratio, from columns (10) and (11).

Column (15).—Approximate morphological type. The convention is that of the RCBG, where -2 corresponds to an S0 and 5 corresponds to an Sc type of galaxy. In most cases these come from the RCBG, although in some cases we have classified the galaxies on the basis of either the plates of Adams (1977) or those of the PSS.

Column (16).—Nuclear radio continuum flux density at 1415 MHz. Fluxes are taken from de Bruyn and Wilson (1976) for the Markarian Seyferts and from van der Kruit (1971) for the others. In a few cases fluxes were taken from preliminary measurements with the very large array by B. B. and T. M. H.

Column (17).—Profile shapes (see § IVc). Absorption lines were detected in three galaxies. The optical depths, H I column densities, absorption redshifts, and full line widths are given in Table 2. The optical depths τ_{HI} are given by

$$\tau_{\text{HI}} = -\ln(1 + \Delta S/S_{1415}), \quad (3)$$

where ΔS is the maximum depth of the line and S_{1415} is the nuclear continuum flux density at 1415 MHz. (It is implicitly assumed that the H I is absorbing continuum from the nuclear region. Indeed, absorption lines are seen only in those Seyferts containing a strong and extended nuclear continuum source.) The H I column density N_{HI} (cm^{-2}) is calculated from

$$N_{\text{HI}} = 1.8 \times 10^{18} T_{\text{spIn}} \Delta v_{\text{ch}} \sum \tau_{\text{HI}}(v), \quad (4)$$

where a spin temperature $T_{\text{spIn}} = 100 \text{ K}$ is assumed and $\tau_{\text{HI}}(v)$ is the optical depth in each channel.

IV. INTEGRATED H I CHARACTERISTICS

In the discussion below we emphasize the results obtained for the 25 detected galaxies listed in Table 1. In this sample we select against galaxies with small H I mass, extremely broad H I line widths, or H I redshifts disagreeing with measured optical redshifts by more than $\sim 800 \text{ km s}^{-1}$ (which hence lie near or beyond the edge of our receiver bandpass).

a) Redshifts

The generally "normal" profile shapes and available spatial maps of H I in Seyfert galaxies both strongly indicate that the bulk of the detected H I lies outside of nuclear regions. Thus the H I redshift would seem to be a reliable indicator of Hubble distance (much as stellar absorption features are in the optical spectrum).

A comparison of our H I redshifts with the optical nuclear redshifts should bear on the question of non-cosmological redshifts arising in these active nuclei and perhaps also in quasars, since Weedman (1976), van den Bergh (1975a), and Osterbrock (1977), among others, have pointed out the spectral similarities

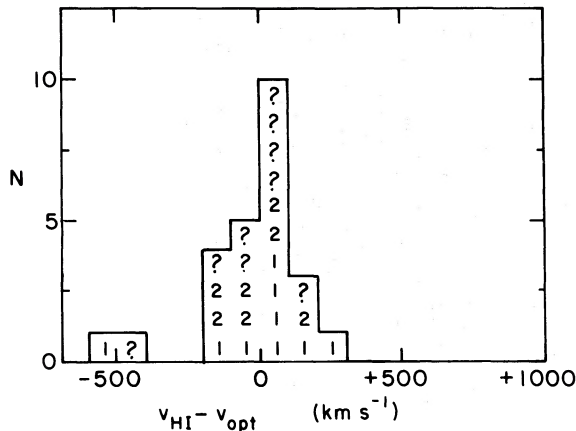


FIG. 2.—Histogram of the differences between the published optical redshift and our measured H I redshift for all galaxies in our sample with detected H I in emission. 1, 2, or ? refers to Seyferts of spectroscopic type 1 or 2, or of questionable status, respectively.

between Seyfert galaxies of type 1 (narrow, forbidden and wide, permitted optical lines) and quasars.

Figure 2 is a histogram of the differences between the optical and H I emission redshifts. Two results are obvious. First, there is no large or statistically significant systematic difference between the optical and H I redshifts. Second, the dispersion of redshifts about $v_{\text{opt}} = v_{\text{HI}}$ is clearly larger than for normal galaxies. Lewis (1975) finds that, for normal galaxies, $\Delta v_{\text{rms}} = \langle (v_{\text{HI}} - v_{\text{opt}})^2 \rangle^{1/2} \approx 45 \text{ km s}^{-1}$, while we find $\Delta v_{\text{rms}} \approx 150 \text{ km s}^{-1}$ for our Seyferts.

The large dispersion between radio and optical redshifts requires some interpretation. Optically, velocities are usually determined from the brightest part of the line profile, i.e., the “peak velocity.” The H I velocity, on the other hand, is determined differently and represents an average of the center of H I mass and the mean of the profile edges. Optical lines are often asymmetric and much broader than the H I lines (especially for type 1 Seyferts). These differences in determining v may explain the redshift discrepancies in Seyferts.

The overall agreement of nuclear and disk redshifts strongly indicates no evidence for any systematic non-cosmological redshifts larger than $\sim 100 \text{ km s}^{-1}$ in Seyfert nuclei.³ The Seyfert galaxy 3C 120 is a particularly noteworthy case. If it is at the distance implied by its optical redshift, then the apparent motion of radio continuum components in its nucleus is several times the speed of light (Cohen *et al.* 1977). Attempts to detect an H I line at NRAO and NAIC were unsuccessful because of the baseline curvature

³ The situation here is entirely analogous to the detection of normal stellar absorption lines in the “fuzz” surrounding a quasar or BL Lacertae-type object (e.g., Miller, French, and Hawley 1978). The fact that both the disk H I gas and the excited nuclear gas have the same redshift in Seyfert galaxies rules out models in which an anomalous redshift is produced only under exotic conditions prevailing in an active nucleus. It does not rule out models in which the anomalous redshift prevails throughout an entire galaxy.

caused by the presence of strong continuum radiation in the beam. For instance, using the 91 m telescope, we attempted OFF-ON observations of both 3C 105 and 3C 120, whose fluxes and declinations are very similar. The spectrum of 3C 105 was scaled by $S_{1420}(3C 120)/S_{1420}(3C 105)$ and subtracted from the spectrum of 3C 120. No statistically significant features of greater than 5 mJy appear in emission or absorption in the resulting spectra.

b) Integrated H I Mass

With the assumption of no H I line absorption, the total H I mass is directly proportional to the H I line flux and the distance squared. In order to circumvent the distance dependence of the H I mass, however, we will discuss the distribution of the ratio $\mathfrak{M}_{\text{HI}}/L_{\text{pg}}$.

A plot of $\mathfrak{M}_{\text{HI}}/L_{\text{pg}}$ versus morphological type for the detected galaxies is shown in Figure 3. Also indicated are mean values and ± 1 standard deviation ranges in the value of $\mathfrak{M}_{\text{HI}}/L_{\text{pg}}$ for normal galaxies of various types taken from Balkowski (1973). These values have been scaled by a factor of 1.3 to adjust the Nançay H I fluxes to the standard NRAO scale, as discussed by Balkowski. One striking feature seen in the figure is the large dispersion, as compared to normal galaxies, of $\mathfrak{M}_{\text{HI}}/L_{\text{pg}}$ for the Seyfert galaxies of a given Hubble type. The three galaxies with the largest $\mathfrak{M}_{\text{HI}}/L_{\text{pg}}$ values are Mrk 3, Mrk 348, and Mrk 463; these in fact lie above the extreme values observed in the *entire* sample of Balkowski. In contrast, the $\mathfrak{M}_{\text{HI}}/L_{\text{pg}}$ values are unusually low in the cases of NGC 1068, NGC 3516, NGC 4235, NGC 7469, and Mrk 231 when compared to the Balkowski sample.

Khachikian and Weedman (1971) suggested a possible correlation between the spectroscopic properties of Seyfert nuclei and the appearance of the galactic disk in the sense that no type 2 Seyferts have conspicuous spiral structure. If such were the case, we might expect type 2 Seyferts to have systematically different $\mathfrak{M}_{\text{HI}}/L_{\text{pg}}$ values than type 1 Seyferts. We do not, however, find this to be the case.

The few extreme values of $\mathfrak{M}_{\text{HI}}/L_{\text{pg}}$ seen in Figure 3 are of considerable interest. It is possible but, as best we can ascertain, very unlikely that measurement errors affecting \mathfrak{M}_{HI} , L_{pg} , and/or the morphological classification may account for the deviant points in the figure. Sources of error in the determination of \mathfrak{M}_{HI} and L_{pg} have already been mentioned. While the estimation of morphological type is fraught with difficulties (e.g., Adams 1977), note that mistakes of one or two Hubble classes cannot account for the observed anomalies in most cases.

We have investigated the possibility that luminosity from the nuclear regions strongly biases both the average and extreme values of $\mathfrak{M}_{\text{HI}}/L_{\text{pg}}$. To properly correct $\mathfrak{M}_{\text{HI}}/L_{\text{pg}}$ for the nuclear magnitudes requires very careful multiaperture photometry. The estimates of nuclear luminosities given in Table 3 are averages of values based on various methods (de Vaucouleurs and de Vaucouleurs 1972, 1973; Penston *et al.* 1974; Weedman 1973). Subtraction of the nuclear magnitudes for the galaxies in Table 3 does not result in any

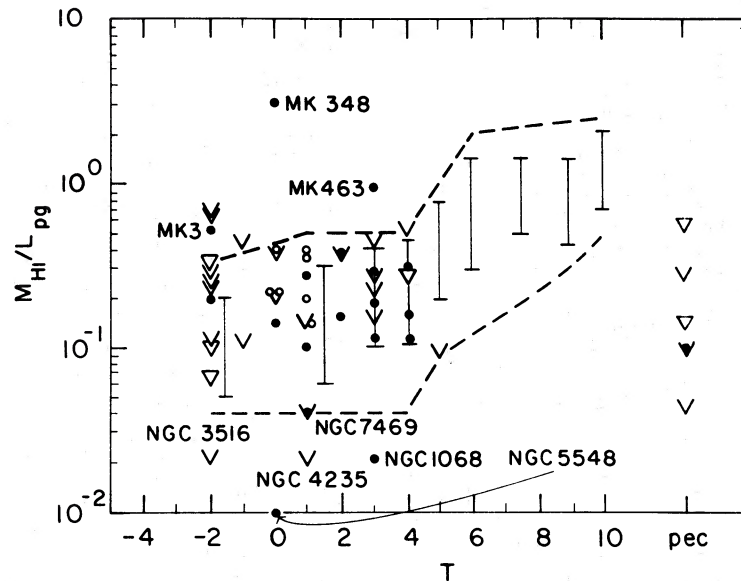


FIG. 3.—The ratio of H I mass to photographic luminosity ($\mathfrak{M}_{\text{HI}}/L_{\text{pg}}$, in solar units) plotted versus galaxy type (T). T is given according to the system in the RCBG ($-5 = E$, $-1 = S0$, $1 = Sa$, $3 = Sb$, $5 = Sc$). Seyfert galaxies are indicated by filled circles for detections and by V for nondetections, while questionable Seyfert galaxies are indicated by open circles for detections and by triangles for nondetections. The bars indicate means and standard deviations, while the dashed lines indicate extreme values of $\mathfrak{M}_{\text{HI}}/L_{\text{pg}}$, for galaxies of various types in the sample of Balkowski (1973).

major changes in Figure 3. Hence we conclude that nuclear contributions to L_{pg} are not the cause of the extreme values of $\mathfrak{M}_{\text{HI}}/L_{\text{pg}}$.

The anomalously large values of $\mathfrak{M}_{\text{HI}}/L_{\text{pg}}$ apparently associated with Mrk 3 and Mrk 463 might be thought to be related to contributions to the H I line flux from nearby galaxies within the antenna beam. However, the galaxy 6' SE of Mrk 463 would be expected to contribute less than 10% of the observed flux. A similarly small contribution is expected from the spiral galaxy 6.5' NNE of Mrk 3. Mrk 348 is definitely not confused. The observations discussed below indicate that the observed H I is all associated with Mrk 348, albeit distributed over a larger scale than expected. The H I flux of Mrk 463 is relatively uncertain and may contribute to its anomalous $\mathfrak{M}_{\text{HI}}/L_{\text{pg}}$ ratio.

Several remarks concerning those Seyfert galaxies that are apparently deficient in H I can be made. First, Gallagher, Faber, and Balick (1975) and Knapp *et al.* (1977) suggest that typical values of $\mathfrak{M}_{\text{HI}}/L_{\text{pg}}$ are substantially lower for early-type galaxies (specifically S0's) than the value we adopt from Balkowski (1973) in our Figure 3. If this is the case, then galaxies such as NGC 3516 and NGC 5548 are about average and other early-type galaxies such as Mrk 352, NGC 4670, Mrk 176, and Mrk 198 are excessive in their values of $\mathfrak{M}_{\text{HI}}/L_{\text{pg}}$ relative to normal galaxies. Note that errors in galaxy morphological classification, especially for cases with very bright nuclei, can be significant in the early-type region of Figure 3.

Second, an intriguing possibility that the "missing" H I exists in molecular form is suggested by the recent results of Rickard *et al.* (1977). NGC 1068, a Seyfert

galaxy shown in Figure 3 with an anomalously low value of $\mathfrak{M}_{\text{HI}}/L_{\text{pg}}$, was one of six galaxies in which Rickard *et al.* detected CO emission at $\lambda = 2.6$ mm. Assuming the chemical abundances in NGC 1068 to be about the same as those in the Galaxy, they estimate the mass of molecular hydrogen to be $\mathfrak{M}_{\text{H}_2} \approx 5\text{--}36 \times 10^9 \mathfrak{M}_{\odot}$. The detected CO lies within 3 kpc of the nucleus. In contrast, we estimate \mathfrak{M}_{HI} to be only $\sim 3 \times 10^9 \mathfrak{M}_{\odot}$, and we find that a substantial part of the H I mass lies well outside the nuclear vicinity and

TABLE 3
FRACTIONAL BLUE LUMINOSITY OF
SEYFERT NUCLEI

Galaxy	$L_{\text{nuc}}/L_{\text{tot}}$
Mrk 1	0.50
NGC 1068	0.04
NGC 1275	0.07
NGC 1566	0.03
3C 120	0.65
Mrk 3	0.20
Mrk 79	0.33
Mrk 10	0.10
NGC 3227	0.03
NGC 3516	0.14
NGC 4051	0.02
NGC 198	0.50
NGC 4151	0.18
Mrk 231	0.58
Mrk 273	0.25
NGC 5548	0.21
Mrk 298	0.58
NGC 6814	0.04
NGC 7469	0.25

perhaps in the bright outer ring around NGC 1068 (see below). If the molecular hydrogen were to be dissociated, then we would measure $\mathfrak{M}_{\text{H I}}/L_{\text{pg}}$ between 0.06 and 0.26. The average value of $\mathfrak{M}_{\text{H I}}/L_{\text{pg}}$ for galaxies of morphological type Sb, such as NGC 1068, is 0.21. We note, however, that it is not at all clear how the atomic hydrogen in the galaxy has been bound into molecular form and removed to the inner regions of the galaxy.

The hypothesis that, for the other Seyferts with low $\mathfrak{M}_{\text{H I}}/L_{\text{pg}}$, the missing H I is in molecular form cannot be tested at present. The predicted CO emission-line intensity is far below the present detection limits of existing millimeter systems. It is noteworthy, however, that most galaxies in which CO has been detected have active nuclei. Assuming the relationship between CO column density and $10\ \mu\text{m}$ luminosity suggested by Rickard *et al.*, values of $\mathfrak{M}_{\text{H}_2}$ predicted for the H I "deficient" galaxies NGC 7469, NGC 5548, and NGC 3516 are 30, 10, and $3 \times 10^9 \mathfrak{M}_{\odot}$, respectively. If dissociated, the resulting values of $\mathfrak{M}_{\text{H I}}/L_{\text{pg}}$ for these galaxies would be normal.

c) Line Shapes and Widths

We have classified the line shapes of the bright lines into a few categories (see col. [17] of Table 1). Those profiles showing the usual central minimum between two peaks are denoted as 2ps or 2pa, depending upon whether the line shapes are symmetric or asymmetric. (In general, asymmetric lines are characterized by "horns" whose relative fluxes differ by at least a factor of 2.) Those profiles with a single central maximum are classified as 1ps or 1pa; the symmetry designation is assigned subjectively by inspection of the profile. Finally, complex profiles not easily categorized as any of the above are listed as cpx.

A comparison between profile shape and other integrated properties of the Seyfert galaxies shows that peculiar line shapes and other unusual properties are correlated. Of the nine galaxies with abnormal values of Δv_{tot} and/or $\mathfrak{M}_{\text{H I}}/L_{\text{pg}}$, four are of type cpx, four are of type 1ps, and one is of type 2ps. Of the remaining detected galaxies, none is cpx, four are 1p, seven are 2ps, and five are 2pa. Higher-spatial-resolution observations of selected galaxies with exceptional or peculiar profile shapes are being planned for the future in order to study possible departures from circular motion.

About one-third of the Seyfert galaxies exhibit significant differences from the canonical double-horned H I profile shape. The most deviant profiles are characterized by either excessive total width, conspicuous line wings extending from ± 100 to as high as $\pm 500\ \text{km s}^{-1}$ from the line centroid (but note that still wider wings cannot be separated from spectral-baseline curvature in our limited bandpass), gross asymmetries in the brightest features of the line profile, or all of the above. Deviant profiles of this sort are exhibited by AKN 253, NGC 3227, NGC 7469, Mrk 3, Mrk 590, and Mrk 541. Wide wings may be present, but obscured by noise, in many of the

other galaxies as well. Roberts and Steigerwald (1977) have recently discussed the putative high-velocity wings of NGC 1068, which they suggest may be attributed to radial gas motions. When compared to profiles of other Seyfert galaxies, however, we find that NGC 1068 is not particularly unusual in its profile shape or width, and we do not categorize its shape as abnormal.

Brief remarks about specific galaxies with exceptional profile shapes are in order. First, Mrk 3 exhibits remarkably broad and irregular features over a $\sim 700\ \text{km s}^{-1}$ spectral region. In many respects Mrk 3 resembles NGC 1275 (3C 84); for instance, ionized gas is observed over large portions of its non-nuclear regions (Adams 1977; Neugebauer *et al.* 1976). Mrk 3 is the most likely of the observed galaxies to be a candidate for H I motions disturbed by nuclear activity, although the possibility exists that the companion galaxy discussed above makes a significant contribution to the profile width. Second, both NGC 3227 and NGC 7469 are members of double and very likely interacting galaxy systems. The NGC 3226/3227 system has been discussed by Rubin and Ford (1968). The companion to NGC 7469 is a peculiar Scd galaxy, IC 5283. The redshift of IC 5283 is virtually identical to that of NGC 7469, and its projected distance is 30 kpc (1.2 NNE) from NGC 7469 (Burbidge, Burbidge, and Prendergast 1963). Observations made on the 305 m telescope centered at the positions of both galaxies reveal that the H I is probably distributed in a common envelope. Considering only the H I that can be reliably associated with NGC 7469, we would thus derive a value of $\mathfrak{M}_{\text{H I}}/L_{\text{pg}}$ a factor of 2 or more lower than the value listed in Table 1 and displayed in Figure 3. The peculiar shapes of the H I profiles of NGC 3227 and NGC 7469 are thus quite possibly unrelated to any nuclear activity.

AKN 253 exhibits a rather strange profile. While AKN 253 was described by Weedman (1977) as a Seyfert galaxy (and so was included in our observations), subsequent observations by Osterbrock and Phillips (1977) have revealed that its nuclear spectrum is qualitatively similar to that of the normal galaxy M51.

Mrk 590 is noted by Adams (1977) to have an E-type companion located only some 43 kpc (projected) away. It is thus likely that the extreme width of the profile ($\sim 1000\ \text{km s}^{-1}$ corrected for inclination) is due primarily to an interaction with the companion. Although the signal levels for Mrk 590 are not high enough for one to be certain, it would appear that the wings in the profile are symmetric, unlike the cases for the other interacting systems NGC 7469 and 3227.

Adams's (1977) photograph of Mrk 541 shows it to be a thin partial ring surrounding a bright inner disk, not unlike NGC 1068. Whether, as in the case of NGC 1068 (see § Va), this disturbed H I is associated with the ring cannot be ascertained from our data. The extreme width of the H I profile of Mrk 541, $\sim 1000\ \text{km s}^{-1}$, is noteworthy and may be the widest H I line ever detected.

Figure 4 is a histogram of line widths taken from

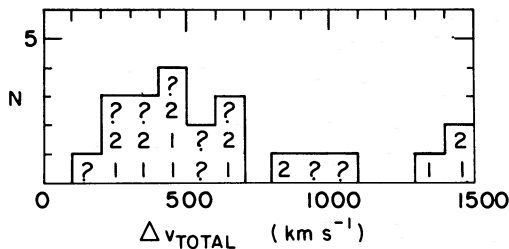


FIG. 4.—Histogram of total H I profile width corrected for inclination for detected galaxies (see text). 1, 2, or ? refers to Seyferts of spectroscopic type 1 or 2, or of questionable status, respectively.

column (5) of Table 1 (only for those galaxies with inclinations exceeding 20°). The mean value of the sample is roughly 550 km s^{-1} . While this value is larger than that typical of normal galaxies, the majority of Seyfert galaxies do not have excessively broad profiles.

d) H I Absorption

Finally, we discuss the three Seyfert galaxies in which H I absorption-line features are observed. Two of the line detections (in Mrk 6 and Mrk 231) are certain, and the other (in NGC 5548) is probable.

The H I absorption feature in Mrk 231 is the broadest extragalactic H I absorption feature (240 km s^{-1}) yet detected. Interestingly, the H I absorption feature occurs within 200 km s^{-1} of the optical emission-line redshift at $12,430 \text{ km s}^{-1}$, while attempts to detect any H I feature at the velocity of the optical absorption-line velocity ($cz = 7900 \text{ km s}^{-1}$) were unsuccessful. The H I absorption feature in Mrk 6 has been reported previously (Burke and Haschick 1978).

Both Mrk 6 and Mrk 231 are notable in several respects other than in their H I absorption features. Both have known extended radio continuum structure around the nucleus at $\lambda = 21 \text{ cm}$ (de Bruyn and Wilson 1976). This suggests that the absorbing H I region is near, but not coincident with, the nucleus and may be associated with the inner part of the disk. In corroboration of this conclusion are the H I column densities listed in Table 2. These values are typical for column densities of disk-related H I emission lines from normal galaxies (Balkowski 1973).

The velocity of the H I absorption feature in Mrk 6 is blueshifted by only 65 km s^{-1} and that in Mrk 231 is redshifted by $\sim 200 \text{ km s}^{-1}$ relative to their respective published optical emission-line redshifts. In view of the typical dispersion in radio and optical redshifts shown in Figure 2 and the widths of the optical and H I absorption lines, such differences in redshifts are probably not significant.

The absorption feature in NGC 5548 is a 3σ feature, and we deem its detection probable. A 21 cm synthesis map of NGC 5548 (van der Kruit 1971) shows two small radio components of nearly equal flux density ($\sim 30 \text{ mJy}$) separated by ~ 1.7 in the east-west direction. The more easterly component is coincident with

the center of the galaxy, and the other is located in the outer periphery of the disk. The relatively narrow line width ($\sim 35 \text{ km s}^{-1}$) suggests that the absorption arises in the galactic disk. Moreover, the derived H I column density is consistent with this interpretation. The redshift of the absorption line, however, is 450 km s^{-1} less than that of the H I emission. This argues for an interpretation in which the absorbing H I has been ejected from the galaxy. Observations made with the $3'3$ beam of the 305 m dish indicate that the absorption feature, if real, appears more strongly against the nuclear radio source.

The very deep minimum seen in NGC 7469 is of unquestionable statistical significance. However, the interpretation of the minimum as an absorption feature is ruled out. Since the only radio source against which H I could be seen in absorption is located in the nucleus of NGC 7469, a true absorption line ought to appear most strongly in the direction of NGC 7469. Our observations indicate, however, that the minimum is equally prominent in the direction of IC 5283. Thus the feature seems to be related to a lack of H I rather than to the presence of absorption.

One of the original motivations of this project was to pursue the possibility that Seyfert nuclei which exhibit strong permitted and forbidden Fe II emission lines and nuclear radio continuum components might also exhibit strong H I absorption lines. The presence of the Fe II lines is often taken as evidence that regions of very high density ($\gtrsim 10^7 \text{ cm}^{-3}$) exist. H I absorption should be readily detectable from such dense regions, provided they are located along the line of sight to the radio continuum source.

Our program included four Seyfert nuclei in which a known nuclear radio source and permitted iron lines of moderate intensity—Fe II ($\lambda 5190 + \lambda 5320$)/ $H\beta > 10\%$ —are detected (D. E. Osterbrock, private communication). Of these, only one shows any evidence of absorption, to wit, NGC 5548. The other Seyfert galaxies in which H I absorption lines are definitely seen do not exhibit Fe II permitted lines. It does not appear that Fe II emission is either a necessary or a sufficient condition for H I absorption against a continuum source in the nucleus.

V. H I MAPS

The $3'3$ beam of the 305 m telescope is sufficiently small that H I mapping was feasible for several galaxies.

a) NGC 1068

NGC 1068 is one of the closest and brightest (and therefore best observed) of all Seyfert galaxies. Excellent photographs of this galaxy, its nuclear regions, and outer rings are available in *The Hubble Atlas* (Sandage 1961). Photometric observations of the galaxy are available (Hodge 1968; D. E. Brownlee, J. P. Cassinelli, and P. W. Hodge, unpublished). NGC 1068 at optical wavelengths shows a bright disk with tightly wound spiral arms (dimensions, $\sim 1.5 \text{ EW}$ by $2' \text{ NS}$) and a large but luminous outer

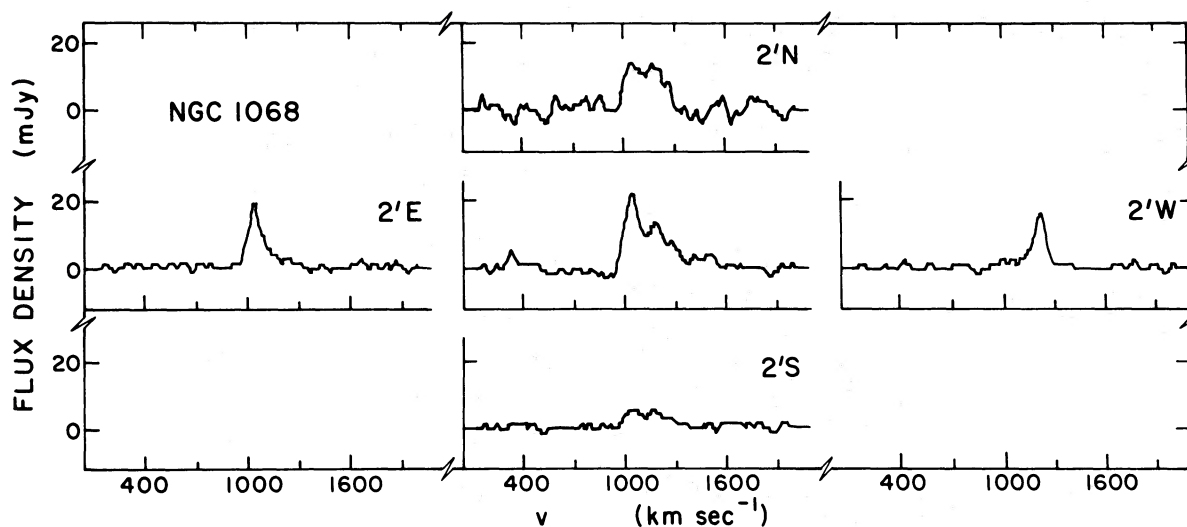


FIG. 5.—H I profiles for NGC 1068 observed with a $\sim 5' \times 3'$ beam at Arecibo. The velocity and flux scales are given in the figure. The profiles are oriented as on the sky, and their positions relative to the center of NGC 1068 are given.

ring (6' EW by 4' NS) oriented more or less along the galaxy *minor* axis.

Photographic photometry by Brownlee *et al.* shows rapid changes of major axis position angle with radius. The position angle of the disk major axis varies from 0° in the nuclear regions ($r \lesssim 10''$) to 90° at $r \approx 30''$ and then precipitously reverts to 0° at $45'' \lesssim r \lesssim 100''$. At about $r \approx 100''$ the arms become very faint, and we deem this the galaxy edge. The brightness increases again in the outer rings. Between the galaxy edge and the rings the position angle of the major axis changes smoothly from 0° to -90° .

In most normal galaxies and in the Seyfert galaxy NGC 4151 (Bosma, Ekers, and Lequeux 1977), the extent of the H I distribution is larger than that of the optical luminosity distribution and the $\mathfrak{M}_{\text{HI}}/L_{\text{DGE}}$ ratio increases with radius, especially beyond the edge of the nuclear bulge. Moreover, the dynamical axis of the H I is aligned with the minor axis of the optical galaxy.

The present Arecibo observations, shown in Figure 5, clearly show that the scale size of the H I distribution is larger than that of the optical light profile in NGC 1068. These observations were made at nine points defining a 4' by 4' grid centered on the nucleus. The four grid points not shown in Figure 5 contained no signal not attributable to sidelobe effects. The scale sizes determined in these measurements are consistent with the sizes of the outer disk or perhaps even that of the outer ring. Moreover, the dynamical axis of the H I, as best we can determine, is perpendicular to the galaxy minor axis measured at the galaxy edge near $r \approx 100''$ and, of course, is aligned with its minor axis at $30'' \lesssim r \lesssim 40''$ (the inner galaxy) and at $r \gtrsim 3'$ (the outer ring).

A word of caution is in order concerning the H I results. NGC 1068 must be observed at zenith angles exceeding $\sim 18^\circ$ at Arecibo. At these zenith angles the feed illuminates the upper lip of the reflector and some

adjacent ground. As a result, the beam pattern is degraded and the system temperature is relatively large for the present observations of NGC 1068. The main-beam major axis increases to $\sim 5'$ in the NS direction, and the sidelobe levels increase from 10% to perhaps 15%. Because of limited observing time in our program, we were unable to measure the beam distortion accurately, and no attempt to correct for it has been made. Pointing was checked often with respect to 3C 71, the strong nuclear radio source in NGC 1068. Despite these difficulties, the direction of the H I dynamical axis and, to a lesser extent, the estimate of the H I scale size should not be seriously in error.

It is interesting to compare the H I dynamics in NGC 1068 to the optically observed kinematics (Walker 1968). Walker's study is based on optical spectra of the ionized gas out to angular distances of $40''$ from the nucleus. He interprets the optical spectra as indicative of both expansion and rotation for $r \lesssim 25''$ and of pure rotation about a dynamical axis in position angle -35° for $25'' \lesssim r \lesssim 40''$. This axis is not consistent with any of the photometric minor axes measured in the inner $40''$ of the galaxy, nor does it agree with the H I rotation axis as measured over considerably larger scales.

Additionally, virial masses computed from the neutral and ionized gas are remarkably disparate. Walker derives $\log(\mathfrak{M}/\mathfrak{M}_\odot) \approx 10.1$ (adjusted to $H_0 = 50 \text{ km s}^{-1} \text{ Mpc}^{-1}$) for solid-body rotation, or 9.8 for a rotating spheroid of axial ratio $c/a = 0.10$. This estimate pertains to the inner $40''$ (4 kpc) of the galaxy. On the other hand, the total mass based on the 43 m H I profile and equation (2) yields $\log(\mathfrak{M}/\mathfrak{M}_\odot) \approx 11.8 \pm 0.3$ for an assumed H I diameter of 6'—a factor of 100 larger than the optical estimate! This difference is at least a factor of 5 larger than might be expected for the extreme case of a galaxy with no central mass concentration.

One or both of the derived indicative masses must be in error. Evidence of noncircular motions has been noted both by Walker in his optical measurements and by Roberts and Steigerwald (1977) in the H I profile. Nonetheless, the present crude H I map and the very typical value of \mathfrak{M}_i/L_{pg} derived from our H I observations support the contention that the majority of the H I is involved in a pattern of simple rotation.

b) NGC 3227

We noted earlier that NGC 3226 and 3227 form an interacting system. The H I map made at Arecibo appears to show some sort of interaction that disturbs the H I kinematics. The region was mapped at five points over a regular 3' by 3' grid centered on the nucleus of NGC 3227. The results are displayed in Figure 6.

The H I profiles suggest rotation about a roughly EW axis, with the gas approaching on the north side. This result is critically dependent, however, upon the reality of the weak emission wing extending down to $\sim 500 \text{ km s}^{-1}$ seen in the profile taken 3' N of the nucleus. This weak emission is exhibited in the 91 m profile as well (see Fig. 1).

Rubin and Ford (1968) studied the kinematics of the excited gas in NGC 3227 and obtained results consistent with the above picture. NGC 3226 is located $\sim 2'$ NNE of NGC 3227, and the two are connected by a luminous bridge or spiral arm with a velocity of $\sim 500 \text{ km s}^{-1}$. Thus the low-velocity gas seen in the profile taken 3' N presumably represents gas associated with this bridge. We see no evidence for any H I bound to NGC 3226 ($v \approx 1350 \text{ km s}^{-1}$).

Rubin and Ford's optical rotation curve extends out to $r \approx 70''$ ($\sim 8 \text{ kpc}$ if the system is at 22 Mpc). Within this region they derive $\mathfrak{M}_i \approx 5 \times 10^{10} \mathfrak{M}_\odot$. In contrast, we detect H I out to $\sim 3'$ and derive $\mathfrak{M}_i \approx 7 \times 10^{11} \mathfrak{M}_\odot$ on the basis of our 43 m profile.

Clearly, the H I in the outermost regions of this system is very disturbed; therefore, our estimate of \mathfrak{M}_i is too large.

c) NGC 4670

NGC 4670 has been suspected to be a Seyfert galaxy by de Vaucouleurs (1968), but spectra obtained by DuPuy (1970) failed to confirm this classification. It is an S0/a galaxy with several peculiar characteristics (Arp 1966).

The optical size of NGC 4670 (1'.8) is considerably smaller than the size of the Arecibo beam. Nonetheless, a five-point map at the galaxy center and at 3' offsets in the cardinal directions shows some indication of partial resolution. The H I size appears to be similar to the optical size of the galaxy, with an H I rotation axis oriented approximately NS. As best as we can determine, there is nothing unusual about the H I properties of NGC 4670 in spite of its peculiar optical morphology and possible Seyfert galaxy status.

d) Mrk 348

This galaxy is revealed by Adams's (1977) photographs to be an early-type spiral with a disk of extremely low surface brightness. Our 91 m observations indicate the extraordinarily large value for $\mathfrak{M}_{H I}/L_{pg}$ of ~ 3.3 .

The observations of Mrk 348 made with the 305 m telescope clearly show the H I in this galaxy to be extended some 5'-6', a value remarkably greater than the optical diameter of only 1'.5. If Mrk 348 is at its cosmological distance, these angular diameters correspond to $\sim 40 \text{ kpc}$ for the optical diameter and $\sim 150 \text{ kpc}$ for the H I diameter! Since Mrk 348 is seen nearly face-on, no information on the H I kinematics was obtained; i.e., the velocity centroid of the line was independent of position in the galaxy. High-spatial-resolution observations of the H I associated

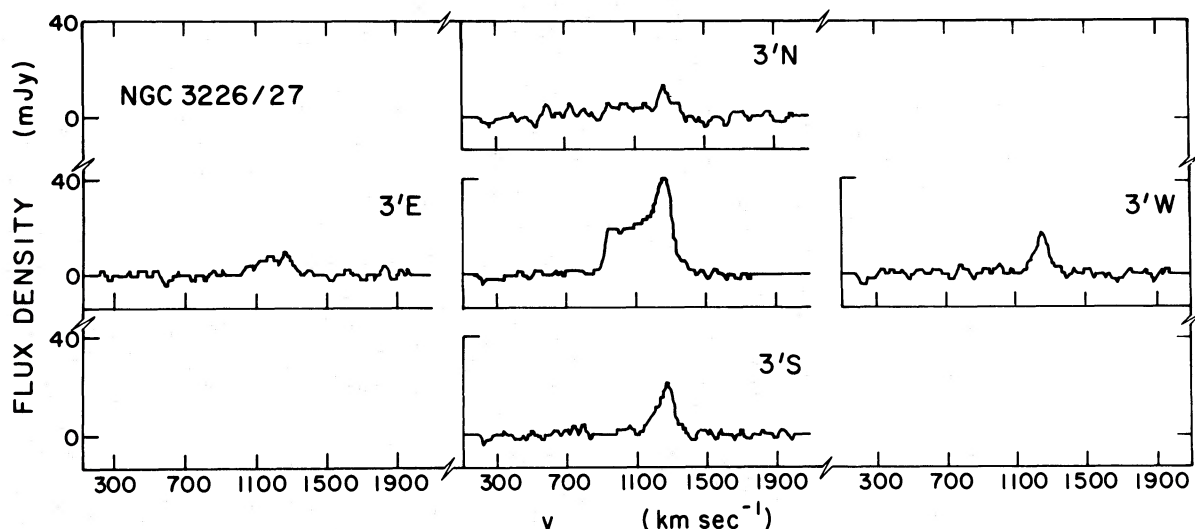


FIG. 6.—H I profiles for NGC 3226/3227 observed with a 3:3 circular beam at Arecibo. The velocity and flux scales are given in the figure. The profiles are oriented as on the sky, and their positions relative to the center of NGC 3227 are given.

with this galaxy are planned for the near future. Mrk 348 bears a strong resemblance to the galaxy PKS 1718-649 described by Fosbury *et al.* (1977). This latter galaxy has a luminous compact nuclear radio source, a Seyfert-like optical spectrum, a very large $\mathfrak{M}_{\text{H I}}/L_{\text{pg}} \approx 1.3$, and very faint spiral arms; but the H I size is unfortunately not known.

We also note the remark of Strom (1977) that observations of other low-surface-brightness spiral galaxies indicate that, as a class, they have bluer than normal disks and very high $\mathfrak{M}_{\text{H I}}/L_{\text{pg}}$ values. Whether the H I in these galaxies is likewise distributed over a large area relative to the optical disk is not mentioned. We discuss some possible implications of the Mrk 348 phenomenon below.

VI. DISK AND NUCLEAR PROPERTIES

Aside from the single wide-band-filter photographic survey of Adams (1977), little is known about the optical properties of Seyfert disks. Although extensive *UBV* photometry of the nonnuclear regions has been done by Dibai and Lyutyj (1971), the reliability of these results has been called into question by the work of Weedman (1973), Penston *et al.* (1974), and de Vaucouleurs and de Vaucouleurs (1972, 1973, and private communication). The difficulty is in properly subtracting the contribution of the bright nucleus from that of the disk. This problem is avoided in the careful *UBV* spot photometry of NGC 1068 by Smith, Weedman, and Spinrad (1972). While their work reveals its disk to have a significant ultraviolet excess relative to a normal Sb galaxy, comparable photometry does not exist for other galaxies in our sample. Since NGC 1068 is characterized by an unusually low value of $\mathfrak{M}_{\text{H I}}/L_{\text{pg}}$, it would be of interest to see whether other Seyfert galaxies also have disks showing an ultraviolet excess.

The original Markarian survey contained a parameter describing the spatial extent of the ultraviolet continuum in each Markarian object (see, e.g., Markarian 1977). We find that all three Markarian Seyferts having unusually large $\mathfrak{M}_{\text{H I}}/L_{\text{pg}}$ (Mrk 3, Mrk 348, and Mrk 463) are spatially *extended* sources of ultraviolet flux (class d or ds). This is true for only three of the 10 Markarian Seyferts with normal $\mathfrak{M}_{\text{H I}}/L_{\text{pg}}$. Taken together with the results for NGC 1068, this may indicate that there is a relationship between abnormal $\mathfrak{M}_{\text{H I}}/L_{\text{pg}}$ and an extranuclear ultraviolet excess in Seyfert galaxies. This relation would *not* be equivalent to the (color, $\mathfrak{M}_{\text{H I}}/L_{\text{pg}}$)-relation found for normal galaxies, however (e.g., de Vaucouleurs 1977), since Seyferts having both high and low $\mathfrak{M}_{\text{H I}}/L_{\text{pg}}$ would seem to have disks which are bright in the ultraviolet. Whether the ultraviolet excesses present in these disks are entirely due to young, hot stars is not clear. Mrk 3 and Mrk 1 have been found to have relatively strong emission lines over much of their nonnuclear regions, and such a situation may occur frequently in type 2 Seyfert galaxies (Neugebauer *et al.* 1976).

Additionally, there is a tendency for Seyfert

galaxies with unusual H I properties (e.g., $\mathfrak{M}_{\text{H I}}/L_{\text{pg}}$, Δv_{tot} , H I absorption) to be morphologically peculiar. Most of the galaxies with low $\mathfrak{M}_{\text{H I}}/L_{\text{pg}}$ values have bright outer rings (NGC 1068, NGC 3516, NGC 5548, NGC 7469). Mrk 463 has a high value of $\mathfrak{M}_{\text{H I}}/L_{\text{pg}}$ and a double nucleus with a single emerging arm. Mrk 348 has an extremely large value of $\mathfrak{M}_{\text{H I}}/L_{\text{pg}}$ and an abnormally faint disk. Mrk 3 has a very large profile width, a large value of $\mathfrak{M}_{\text{H I}}/L_{\text{pg}}$, outer H α filaments, and an inner disk with bright optical emission lines. Mrk 6 has an H I absorption feature and outer H α filaments. Mrk 231 has an extremely broad H I absorption line, a peculiar nuclear spectrum, and one irregular spiral arm. Finally, Mrk 541 has an outer ring and an extremely broad H I profile.

In contrast, galaxies such as NGC 4051, NGC 6764, NGC 6814, Mrk 10, Mrk 79, and NGC 4939 are apparently normal in respect to both their H I properties and their optical morphology. Others exhibit normal H I properties and optical peculiarities. These include NGC 4151 (outer ring), NGC 4670 (see § Vc), and Mrk 1 (emission lines in the inner disk).

Adams (1977) has tentatively classified Seyfert galaxies into a number of broad groups based upon their optical morphology. We find no clear relationship, other than those noted above, between H I properties and his optical classes. In particular, Mrk 6 and Mrk 352, which were classified as possible E galaxies, both have detectable H I. Mrk 231 and Mrk 176 were both classified as "disturbed or interacting systems." Mrk 231 does have an unusually broad H I absorption feature, while Mrk 176 has apparently normal H I properties.

Next we consider relationships between the nuclear activity and the disk properties. In Table 4 we assemble four measures of nuclear activity in those galaxies in which H I detections were made or significant upper limits to $\mathfrak{M}_{\text{H I}}/L_{\text{pg}}$ were established. These measures are the radio luminosity at 1415 MHz, $L_{1415 \text{ MHz}}$ (de Bruyn and Wilson 1976; van der Kruit 1971); the luminosity at 10 μm , $L_{10 \mu\text{m}}$ (Rieke and Low 1972; Young, Knacke, and Joyce 1972); the reddening-corrected H α luminosity, $L_{\text{H}\alpha}$ (Adams and Weedman 1975); and the *U* luminosity, L_{UV} (Adams and Weedman 1975). The galaxies are grouped into those having unusual H I properties (as discussed above) and those with more normal H I properties. The numbers in columns (2)-(5) represent the rank of each galaxy in terms of the corresponding luminosity measures.

It is apparent that there is a strong tendency for those galaxies with the most luminous nuclei to have unusual H I properties. Despite some obvious exceptions where galaxies with luminous nuclei exhibit normal H I properties (e.g., compare Mrk 10 and Mrk 79 to Mrk 348), the tentative implication is that there exists communication of some sort between the nucleus and the disk.

VII. A SPECULATIVE EVOLUTIONARY SCENARIO

We now describe a set of working hypotheses which provide a speculative framework for our observational

TABLE 4
H I PECULIARITIES VERSUS NUCLEAR LUMINOSITIES

GALAXY (1)	RANK				H I PECULIARITY (6)
	$L_{H\alpha}$ (2)	L_{UV} (3)	$L_{10\mu m}$ (4)	$L_{1415\text{ MHz}}$ (5)	
Mrk 348	11	10	...	5	$\mathfrak{M}_{H I}/L_{pg}$ large
NGC 1068	8	2	2	6	$\mathfrak{M}_{H I}/L_{pg}$ small
Mrk 3	4	3	4	3	Δv , $\mathfrak{M}_{H I}/L_{pg}$ large
Mrk 6	1	1	6	4	Broad absorption line
NGC 3516	5	4	...	14	$\mathfrak{M}_{H I}/L_{pg}$ small
Mrk 231	1	2	Broad absorption line
NGC 5548	2	8	7	12	$\mathfrak{M}_{H I}/L_{pg}$ low, absorption line
Mrk 463	1	$\mathfrak{M}_{H I}/L_{pg}$ high
NGC 7469	6	6	3	7	Δv large, $\mathfrak{M}_{H I}/L_{pg}$ small
Mrk 352	9	11	...	> 15	
Mrk 1	9	9	8	8	
Mrk 10	7	5	...	> 13	
Mrk 79	3	7	5	11	
Mrk 391	> 16	
NGC 2782	9	13	
Mrk 176	9	
NGC 3227	12	12	11	16	
NGC 4051	13	14	12	16	
NGC 4151	10	13	10	13	
NGC 4670	15	
NGC 6764	10	
NGC 6814	> 10	> 17	

results. This discussion is meant to stimulate the development of detailed, quantitative models, for which it is *not* intended to be a substitute.

An examination of Figure 3 reveals two interesting points: First, while there is no striking systematic difference in the *mean* $\mathfrak{M}_{H I}/L_{pg}$ for Seyfert galaxies as compared to normal galaxies, the *dispersion* is considerably larger. Second, it is evident that, at least for the galaxies in our program, the range in Hubble type is restricted to types S0–Sc ($T = -2$ to 5). This general result is corroborated by the photographic survey of Adams (1977), which shows a lack or possibly even a total absence of Seyfert galaxies which are ellipticals, very late-type spirals, or irregulars ($T = -6$ to -3 and 6 to 10). Thirty-nine Seyfert galaxies have been classified in the de Vaucouleurs system in the RCBG. Of these, 24, or 62%, are in the range S0–Sa ($T = -2$ to $+1$). This compares to only 21% for normal galaxies in that range in the RCBG. The evidence thus suggests that the presence of a large central mass concentration plus some disk component (the characteristics of early-type spirals) favors the production of a Seyfert nucleus. Van den Bergh (1975*b*) and Gisler (1978) have noted that Seyfert galaxies do not generally occur in the environment of a rich cluster of galaxies. Since recent work by Krumm (1977) and Sullivan and Johnson (1978) suggests that galaxies in clusters have had some large fraction of their disk gas removed, presumably by the hot intra-cluster gas (e.g., Gisler 1976), we speculate that a gaseous disk also aids in the production of a Seyfert nucleus. Such disk H I may arise from a source internal to the galaxy (mass loss from evolved stars) or one external to it (accretion of outlying H I clouds or collision with a gas-rich system).

We suggest that outbursts of nuclear activity may play a central role in recycling gas in early-type galaxies. This is in contrast to ellipticals, in which galactic winds may sweep out all the H I (Faber and Gallagher 1976). That fraction of the mass lost by evolved stars which can lose sufficient angular momentum will be accreted by the nucleus (see Gott and Thuan 1976 for a discussion of turbulent viscosity in disk gas in a spiral galaxy). Since early-type spirals are dominated by a low-angular-momentum component (the central bulge) and have a stronger central mass concentration, we expect them to be most efficient at such a process. Also, the lack of vigorous disk-star formation in such systems means that mass lost by evolved stars will not be quickly recycled into new disk stars. The activity triggered by the accreted gas may involve the formation of any of the exotic objects postulated to exist in galactic nuclei (Saslaw 1974).

The resulting nuclear outburst may be expected to alter the $\mathfrak{M}_{H I}/L_{pg}$ value and the distribution of disk gas in a variety of ways. The models of nuclear activity developed by Sanders and Bania (1976) predict a shock front which propagates out into the disk at several hundred km s^{-1} . This shock ionizes much of the H I, leads to intense star formation in the compressed gas (raising L_{pg} and lowering $\mathfrak{M}_{H I}$), and plows the remaining H I into a ringlike oscillating structure.

In such a picture, a Seyfert galaxy begins as an early-type, gas-rich spiral (Mrk 348) in which nuclear activity has just turned on. NGC 1275 and possibly NGC 7469 may represent galaxies into which H I has been rapidly injected during an encounter with a gas-rich system. During the early phases of nuclear

activity, we expect the H I still to be abundant but to show signs of disrupted kinematics (Mrk 3). Later, $\mathfrak{M}_{\text{HI}}/L_{\text{pg}}$ drops as the disk is ionized (3C 120, Mrk 1). The H I is pushed out into the periphery of the galaxy, which results in an outer ring of star formation (NGC 1068 and NGC 4151; possibly also NGC 3516, NGC 5548, NGC 7469, and Mrk 541). Finally, the nucleus dies out, and we are left with an early-type spiral with gradually reddening colors, fading outer ring, and increasing $\mathfrak{M}_{\text{HI}}/L_{\text{pg}}$. On the other hand, if the nuclear activity is below some threshold luminosity, we expect the disk *not* to be severely disrupted and normal H I properties to prevail (NGC 4051, NGC 6764, and NGC 6814).

We envisage the process outlined above to occur whenever the fractional amount of disk H I climbs above some threshold value. Thus, early in the universe when the stellar mass-loss rate was high, early-type galaxies may have passed through repeated Seyfert episodes. In the current epoch, we would in the case of Mrk 348, for instance, expect that the time required to produce the $3.4 \times 10^{10} \mathfrak{M}_{\odot}$ of observed H I would be $\sim 10^{10}$ years. Thus, except for early in the universe, we expect the Seyfert "duty cycle" to be $\sim 10^8/10^{10} \approx 0.01$. The well-known increase in space density of quasars at high z may in fact be related to the greater frequency of Seyfert galaxies predicted in the early universe, given the extreme similarity between quasars and type I Seyfert nuclei (Weedman 1976).

Finally, it is possible to relate other types of galaxies to this picture. The wide range in $\mathfrak{M}_{\text{HI}}/L_{\text{pg}}$ and its lack of clear dependence upon *UBV* colors in early-type spiral galaxies (e.g., Biegging and Biermann 1977) may simply reflect the status of an early-type spiral as pre- or post-Seyfert (high and low $\mathfrak{M}_{\text{HI}}/L_{\text{pg}}$, respectively). The fact that early-type spirals with detectable H I frequently have this H I in an outer ring (Gallagher 1977; Biegging and Biermann 1977)

ties in nicely with our idea of gas being snowplowed out of the inner disk. Strom (1977) has described a class of H I-rich galaxies of very low surface brightness. These galaxies may be precursors to Seyferts, and it would be interesting to determine their nuclear properties. The X-ray galaxy IC 3576 (Margon *et al.* 1972), Cen A (Whiteoak and Gardner 1971), M82, and other active S0 and Ir II galaxies (Gallagher, Faber, and Balick 1975), all characterized by excessive H I, may represent either pre-Seyferts, cases in which the Seyfert nature of the nucleus is obscured, or related objects following evolutionary tracks that differ in some critical way from those followed by Seyfert galaxies.

Clearly, detailed studies of the nature of the neutral, molecular, and ionized gas, as well as color maps to study star formation rates, are needed for Seyfert and related active galaxies. We hope soon to begin such a program, which may eventually involve high-resolution H I maps, H α photography, spectroscopy, and *UBV* photographic photometry of selected Seyfert galaxy disks.

We thank the operations staffs of the NRAO and NAIC for their extensive help in acquiring and reducing the data. Special thanks are accorded to R. Fisher and B. Stobie of the NRAO and E. Conklin and N. Krumm of the NAIC. R. Schommer ably assisted with some of the 305 m observations. T. Adams, D. E. Osterbrock, B. Burke, S. Grandi, D. Jenner, D. Weedman, and H. French provided data in advance of its publication which proved invaluable in organizing our observing program. This research was partially supported by the Graduate School Research Fund of the University of Washington. Travel support from the NRAO and NAIC is also gratefully acknowledged.

REFERENCES

- Adams, T. F. 1977, *Ap. J. Suppl.*, **33**, 19.
 Adams, T. F., and Weedman, D. W. 1975, *Ap. J.*, **199**, 19.
 Arp, H. C. 1966, *Ap. J. Suppl.*, **14**, 1.
 Balkowski, C. 1973, *Astr. Ap.*, **29**, 43.
 Biegging, J. M., and Biermann, P. 1977, *Astr. Ap.*, **60**, 361.
 Bosma, A., Ekers, R. D., and Lequeux, J. 1977, *Astr. Ap.*, **57**, 97.
 Burbidge, E. M., Burbidge, G. R., and Prendergast, K. H. 1963, *Ap. J.*, **137**, 1022.
 Burke, B., and Haschick, A. 1978, in preparation.
 Cohen, M. H., *et al.* 1977, *Nature*, **268**, 405.
 Davies, R. D. 1973, *M.N.R.A.S.*, **161**, 25P.
 de Bruyn, A. G., and Wilson, A. S. 1976, *Astr. Ap.*, **33**, 351.
 de Vaucouleurs, G. 1968, *A.J.*, **73**, 858.
 ———. 1977, in *The Evolution of Galaxies and Stellar Populations*, ed. B. M. Tinsley and R. B. Larson (New Haven: Yale University Observatory), p. 43.
 de Vaucouleurs, G., and de Vaucouleurs, A. 1972, *Ap. Letters*, **12**, 1.
 ———. 1973, *Cima Eker Dedication*.
 de Vaucouleurs, G., de Vaucouleurs, A., and Corwin, H. G. 1976, *The Second Reference Catalogue of Bright Galaxies* (Austin: University of Texas Press) (RCBG).
 Dibai, E. A., and Lyutyj, V. M. 1971, *Astrofizika*, **7**, 169.
 DuPuy, D. L. 1970, *A.J.*, **75**, 1143.
 Faber, S. M., and Gallagher, J. S. 1976, *Ap. J.*, **204**, 365.
 Fosbury, R. A. E., Mebold, U., Goss, W. M., and van Woerden, H. 1977, *M.N.R.A.S.*, **179**, 89.
 Gallagher, J. S. 1977, in *The Evolution of Galaxies and Stellar Populations*, ed. B. M. Tinsley and R. B. Larson (New Haven: Yale University Observatory), p. 95.
 Gallagher, J. S., Faber, S. M., and Balick, B. 1975, *Ap. J.*, **202**, 7.
 Gisler, G. R. 1976, *Astr. Ap.*, **51**, 137.
 ———. 1978, *M.N.R.A.S.*, in press.
 Gott, J. R., and Thuan, T. X. 1976, *Ap. J.*, **204**, 649.
 Hodge, P. W. 1968, *A.J.*, **73**, 846.
 Khachikian, E. Y., and Weedman, D. W. 1971, *Astrofizika*, **7**, 389.
 ———. 1974, *Ap. J.*, **192**, 581.
 Knapp, G. R., Gallagher, J. S., Faber, S. M., and Balick, B. 1977, *A.J.*, **82**, 106.
 Koski, A. 1976, Ph.D. thesis, University of California, Santa Cruz.
 Krumm, N. 1977, Ph.D. thesis, Cornell University, Ithaca, New York.
 Lewis, B. M. 1975, *Mem. R.A.S.*, **78**, 75.
 Lewis, B. M., and Davies, R. D. 1973, *M.N.R.A.S.*, **165**, 213.
 Margon, B., Spinrad, H., Heiles, C., Tovmassian, H., Harlan, E., Bowyer, S., and Lampton, M. 1972, *Ap. J. (Letters)*, **178**, L77.
 Markarian, B. E. 1967, *Astrofizika*, **3**, 55.
 ———. 1969a, *Astrofizika*, **5**, 443.
 ———. 1969b, *Astrofizika*, **5**, 581.
 ———. 1973, *Astrofizika*, **9**, 5.
 ———. 1977, *Astr. Ap.*, **58**, 139.

- Markarian, B. E., and Lipovetsky, V. A. 1971, *Astrofizika*, **7**, 511.
 ———. 1972, *Astrofizika*, **8**, 155.
 ———. 1973, *Astrofizika*, **9**, 487.
 ———. 1974, *Astrofizika*, **10**, 307.
 Miller, J. S., French, H. B., and Hawley, S. A. 1978, *Ap. J. (Letters)*, **219**, L85.
 Neugebauer, G., Becklin, E. E., Oke, J. B., and Searle, L. 1976, *Ap. J. (Letters)*, **205**, L29.
 Osterbrock, D. E. 1977, *Ap. J.*, **215**, 733.
 Osterbrock, D. E., and Phillips, M. M. 1977, *Lick Obs. Bull.*, No. 764.
 Penston, M. V., Penston, M. J., Selmes, R. A., Becklin, E. E., and Neugebauer, G. 1974, *M.N.R.A.S.*, **169**, 357.
 Rickard, L. J., Palmer, P., Morris, M., Turner, B. E., and Zuckerman, B. 1977, *Ap. J.*, **213**, 673.
 Rieke, G., and Low, F. J. 1972, *Ap. J. (Letters)*, **176**, L95.
 Roberts, M. S. 1975, in *Galaxies and the Universe*, ed. A. Sandage, M. Sandage, and J. Kristian (Chicago: University of Chicago Press), p. 309.
 Roberts, M. S., and Steigerwald, D. G. 1977, preprint.
 Rubin, V. C., and Ford, W. K., Jr. 1968, *Ap. J.*, **154**, 431.
 Sandage, A. R. 1961, *The Hubble Atlas* (Washington: Carnegie Institution of Washington).
 Sanders, R. H., and Bania, T. M. 1976, *Ap. J.*, **204**, 341.
 Saslaw, W. C. 1974, in *IAU Symposium No. 58, Formation and Dynamics of Galaxies*, ed. J. R. Shakeshaft (Dordrecht: Reidel), p. 305.
 Shostak, G. S. 1975, *Ap. J.*, **198**, 527.
 Simkin, S. M. 1975, *Ap. J.*, **200**, 567.
 Smith, M. G., Weedman, D. W., and Spinrad, H. 1972, *Ap. Letters*, **11**, 21.
 Strom, S. E. 1977, in *The Evolution of Galaxies and Stellar Populations*, ed. B. M. Tinsley and R. B. Larson (New Haven: Yale University Observatory), p. 219.
 Sullivan, W. T., III, and Johnson, P. E. 1978, preprint.
 van den Bergh, S. 1975a, *J.R.A.S. Canada*, **69**, 105.
 ———. 1975b, *Ap. J. (Letters)*, **198**, L1.
 van der Kruit, P. C. 1971, *Astr. Ap.*, **15**, 110.
 Walker, M. F. 1968, *Ap. J.*, **151**, 71.
 Weedman, D. W. 1973, *Ap. J.*, **183**, 29.
 ———. 1976, *Quart. J.R.A.S.*, **17**, 227.
 ———. 1977, *Ann. Rev. Astr. Ap.*, **15**, 69.
 Whiteoak, J. B., and Gardner, F. F. 1971, *Ap. Letters*, **8**, 57.
 Young, E. T., Knacke, R. F., and Joyce, R. R. 1972, *Nature*, **238**, 263.
 Zwicky, F., and Herzog, E. 1963, *Catalogue of Galaxies and Clusters of Galaxies* (Pasadena: California Institute of Technology).

BRUCE BALICK, TIMOTHY M. HECKMAN, and WOODRUFF T. SULLIVAN III: Department of Astronomy, University of Washington, Seattle, WA 98195